Received: 4 January 2021 | Revised: 23 August 2021 | Accepted: 12 September 2021

DOI: 10.1002/er.7307

RESEARCH ARTICLE

INTERNATIONAL JOURNAL OF ENERGY RESEARCH WILEY

Dye pH effect on photoelectric parameters of natural photosensitizer pigment extracted from *Alstonia boonei* for dye-sensitized solar cells

Uche E. Ekpunobi[1] | **Solomon I. Ogbuefi**[1] | **Azubike J. Ekpunobi**[2]

[1]Pure and Industrial Chemistry Department, Nnamdi Azikiwe University, Awka, Nigeria

[2]Physics and Industrial Physics Department, Nnamdi Azikiwe University, Awka, Nigeria

Correspondence
Uche E. Ekpunobi, Pure and Industrial Chemistry Department, Nnamdi Azikiwe University, Awka, Anambra State. Nigeria.
Email: ue.ekpunobi@unizik.edu.ng

Summary

The study was carried out to ascertain the effect of pH on sensitizing ability of a natural photosensitizer dye. Natural dye extracted from *Alstonia boonei* (Stool wood) leaves was assessed for its chemical compositions using IR, UV and GC-MS and revealed the presence of many bioactive compounds that promote sensitizing ability. The pH of 100 mL portions of the dye was adjusted to 1.30, 3.00, 5.68 and 6.33, then used to sensitize solar cells fabricated using the screen printing method. These dye-sensitized solar cells (DSSCs) were characterized using UV-spectroscopy, XRD, SEM and solar simulation, from which the I-V properties, fill factor (FF) and efficiency of the cells were determined. The photoelectrical performance of the cells showed an open-circuit voltage (V_{oc}) of 0.490 V, short-circuit current density J_{sc} of 0.67 mA/cm^2, a fill factor (FF) of 0.701 and a conversion efficiency of 0.23% for the DSSC at dye pH 1.30, V_{oc} of 0.469 V, J_{sc} of 3.10 mA/cm^2, an FF of 0.671 and a conversion efficiency of 0.980% for DSSC at dye pH of 3.0, V_{oc} of 0.48 V, J_{sc} of 3.0 mA/cm^2 an FF of 0.673 and a conversion efficiency of 0.969% for DSSC at dye pH 5.63 and V_{oc} of 0.51 V, J_{sc} of 0.33 mA/cm^2, FF of 0.309 and conversion efficiency of 0.052. The cells showed absorption at the UV, visible and near infrared (NIR) with maximum absorption of 1.298, 1.963, 1.413 and 1.589 at lambda maxima (λ_{max}, nm) at 299.50, 307.84, 307.84 and 307.84, respectively, for DSSCs at dye pH values of 1.30, 3.00, 5.63 and 6.33, respectively. Most of the parameters tested showed that there was better conversion efficiency for the cells at a dye pH of 3. This affirms that modifying the pH of sensitizer dyes enhances the absorption capacity and overall cell efficiency.

KEYWORDS

Alstonia boonei, dye, natural dye-sensitized solar cells, pH, photo-electricity, photosensitizers, pigment, renewable energy

1 | INTRODUCTION

In recent times, energy generation has mostly been from fossil fuels and nuclear power. The known limitations of these sources have, however, encouraged stakeholders and researchers to focus on a transition to alternative, renewable, environmentally friendly and safer sources of energy.[1,2] One of such is the dye-sensitized solar cell (DSSC), which has attracted much research interest due to its relatively low cost and environmental friendliness.[3,4] Sensitizer dye plays a very important role in DSSC as it can effectively harvest solar energy from a cell

and convert it to electric power. Black dye, which is ruthenium-based, has enjoyed the most use in DSSC because of its efficiency; however, it is expensive. Furthermore, it is difficult to prepare and not environment friendly. The optimization and use of cheap and available natural dyes are thus the current focus for researchers. Enhancing the sensitizing ability of known dyes are even more revealing in the overall journey to optimization of natural dye-sensitized solar cell (nDSSC) to meet up with or overtake their synthetic dye counterparts.[5-7] Anthocyanin, belatin and chlorophyll are some of the pigments/dyes that have attracted much attention in this area.[8] *Alstonia boonei* extract has been reported to have high molar extinction coefficients in the visible region. However, acidic conditions are known to induce recondensation of acid and favours photo-electrode with high optical densities capable of complete solar absorption within the visible region at 400 to 700 nm.[8,9] The present study thus investigates the pH dependent redox properties on photoelectric parameters of natural photosensitizer pigment extracted from *Alstonia boonei* for DSSCs. The effect of varying the pH of absorption on the absorption maxima was also determined with the hope of improving the sensitizing ability of the light harvesting dye. Solar conversion being a function of photocurrent density (J_{SC}), open-circuit voltage (V_{OC}) and fill factor (FF) implies that improving them will improve cell conversion efficiency.[10,11] The aqueous extract pigment of *Alstonia boonei* is subjected to physical analysis, chemical component analysis and photo-conversion of nDSSCs fabricated with the dye at sensitizer dye pH values of 1.30, 3.0, 5.63 and 6.33 in order to correlate the functions of the extracted pigment constituents with enhanced efficiency at different pH values. The use of natural dye from *Alstonia boonei* in DSSC instrumentation has a significance of being benign, cheap source of dye, abundant availability in developing countries above all expanding the economic viability of *Alstonia boonei*. Hence the objective of this study is to modify the pH of the dye extracts used in preparation of DSSCs, and then test the abilities in enhancing the absorption capacity, the optimized pH and overall cell efficiencies.

2 | MATERIALS AND METHODS

2.1 | Materials

The material used for the research is *Astonia boonei* leaves (stool wood), identified and collected from Awka, Anambra State, Nigeria.

All chemicals and reagents used were commercially available analytical grade. They include distilled/deionized water methanol, 0.01 M HCl, 0.1 M H_2SO_4, 0.3/0.15 M acetyl acetone ammonium heptaoxodichromate (vi) solution, potassium heptaoxodichromate (vi) solution d-titanium (iv) isopropoxide (97%), *n*-titanium (iv) oxide D/SP Solaronix, 0.1 M polyethylene glycol, Triton X-100, dehumidifier and ovum, sonicator, 0.1 M hydrofluoric acid and platinum catalyst T/SP Solaronix.

2.2 | Equipment

The key equipment utilized in the work are UV-visible spectrophotometer (ULTROSPEC 2100 PRO), IR spectroscopy, gas chromatography/mass spectroscopy, scanning electron spectroscopy (SEM), X-ray diffraction machine, solar simulator (model 4200-SCS), screen printer and pH meter (model pHS-25).

2.3 | Dye extraction and characterization

Dye was extracted from *Astonia boonei* leaves by maceration method using distilled water.[12,13] The physical properties were determined, and chemical composition was carried out on the extract using UV-visible spectrophotometer (ULTROSPEC 2100 PRO), IR spectrophotometer (Lasany LI-5500 FTIR) and GC-MS Couple.[14]

2.4 | Fabrication of nDSSCs

The required pH values of the dye (1.30, 3.00 and 5.63) were adjusted and established using a pH meter (model pHS-25). The cell's photoanodes were fabricated using screen printing method before being soaked in the different dye solutions at various pH values for 18 hours. They were later rinsed with distilled water to remove debris, dried and covered with aluminium foil till it was used.[15,16] Samples were taken from these electrodes for morphological studies using X-ray diffraction machine and scanning electron microscope SEM (model PW-100-012/800-07334). The various components of the cell, including the photoanode, counter electrodes, the electrolyte, which is a 0.05 M iodide/triiodide solution (iodolyte Z-100, a product of Solaronix), blue gums and tapes were assembled and the cells were coupled. The DSSCs were irradiated using a solar simulator (model 4200-SCS). The UV absorbance of the various cells at different dye pH values was determined using UV-visible spectrophotometer (ULTROSPEC 2100 PRO) over a wavelength range of 200 to 1500 nm. The resistivity and current-voltage characteristics of the cells were obtained using the four-point probe multi-meter testing system.[16]

The mechanism of reactions that ensued on the DSSC upon irradiation to generate continuous current is summarized as follows[17,18]:

Step 1: The photosensitizer, adsorbed on the surface of the semiconductor, absorbs the incident sunlight and becomes excited from the ground state (S) to the excited state (S^*)

$$S + hv \rightarrow S^*$$

Step 2: The excited electrons are injected into the conduction band of the semiconductor, resulting in the oxidation of the sensitizer (S^+)

$$S^* \rightarrow S^+ + e^-_{CB}$$

Step 3: The oxidized sensitizer (S^+) is regenerated by accepting electrons from the iodide ion

$$S^+ + \frac{3}{2}I^- \rightarrow \frac{1}{2}I_3^- + S$$

Step 4: The triiodide redox mediator diffuses towards the counter electrode and is reduced to iodide.

$$I_3^- + 2e^-_{CE} \rightarrow 3I^-$$

In addition to the forward electron transfer and ionic transport processes, several competing electron loss pathways should be considered.

Step 5: Decay of the dye excited state to the ground state

$$S^* \rightarrow S$$

Step 6: Recombination of the injected electrons with the dye cations

$$S^+ + e^-_{CE} \rightarrow S$$

Step 7: Recombination of the injected electrons with the triiodide redox mediator

$$I_3^- + 2e^-_{CE} \rightarrow +3I^-$$

3 | RESULTS AND DISCUSSION

3.1 | FT-IR measurements

The yield of the extracted dye was 2.38%. It was dark green, light scented, fine crystalline and water-insoluble dye with a density of 1.102 g/cm^3. The chemical component results are presented in Table 1.

The result shows that the dye has strong absorption peaks at the following regions 3600, 3376, 3189, 2953, 2733, 2586, 2386 2292 1964, 1847, not like the broad peaks at the fingerprint regions. The peaks of the absorption suggest the presence of carbonyl, C═O (1840) of carboxylic acid and ester, hydroxyl, O—H (3600-3376) of carboxylic acid, carboxyl, C—O (1358) of ester and carboxylic acid, ═C—H (2953) unsaturated carbon chain.[18-20] The carbonyl, carboxyl and hydroxyl groups present in the extract could be responsible for the improved adsorption ability of dye on TiO_2, hence facilitating the charge transfer.[22]

A remarkable advance in the use of organic dyes for DSC was recently made by groups of scientists.[22,23] Using coumarin or polyene type sensitizers, strikingly high solar to electric power conversion efficiencies reaching up to 7.7% in full sunlight have been achieved. The core discovery of the work is that organic sensitizers with many polyenes are capable of extending solar absorption and hence act as good sensitizers or co-sensitizers. The IR result of the *Alstonia boonei* extract shows that there is a significant amount of dienes and polyene compounds in the dye extract.

3.2 | UV absorbance of the extract

The result of the UV scan of the aqueous dye extract starting from the wavelength of 200 to 900 nm is shown in Figure 1. The result of the UV scan of the aqueous dye extract starting from the wavelength of 200 to 900 nm shows that the dye has absorption peaks of various wavelengths, but absorption maxima occurred at wavelengths 341.0 and 405.1 nm. These peaks are at the visible region, indicating the presence of chlorophyll in the extract. There are also strong absorption peaks at the other visible/UV region of the electromagnetic spectrum (10-780 nm).[23] This shows that the sample can act as a sensitizer or solar collector for DSSC. According to Silverstein et al, a strategy to obtain a broad optical absorption extending throughout the visible and near-IR region will be to use a dye that shows strong from the UV/visible down to near-IR region.[24] This can also be achieved by the use of a combination of two dyes, which complement each other in their spectral features within the area of interest when a single sensitizer is not suitable for this purpose. Such dye cocktails have already been applied to mesoporous TiO_2 films in the form of mixtures of porphyrins and phthalocyanines. The result was encouraging in as much as the optical effects of the two sensitizers were found to be additive. In particular, there was no negative

TABLE 1 Infra-red result of the extract showing the chemical component

S/N	Wave-number (cm^{-1})	Peak area	Inference	Compound class[19-21]
1	720.0373	4.384734	C═C bending	Alkene (di substituted)
2	848.0297	35.9277	C═C bending	Alkene (tri substituted)
3	1358.393	115.5464	O—H bending S═O stretching	Phenol
4	1847.394	268.3387	C—H bending C═O, stretching	Aromatic compound Anhydride
5	1964.173	289.5708	C—H bending	Aromatic compound
6	2291.994	300.1857	C—H, stretching	Alkanes
7	2388.321	435.6663	C═N stretching N═C═O stretching	Nitrile Isocyanate
8	2586.633	345.8663	S—H stretching	Thiol
9	2733.289	328.0796	O—H stretching	Alcohol
10	2953.385	302.9066	N—H stretching	Amine salt
11	3189.018	576.0503	O—H stretching	Carboxylic acid
12	3376.016	229.770	O—H stretching N—H stretching	Ester Primary amine
13	3600.166	675.684	O—H stretching	Alcohol

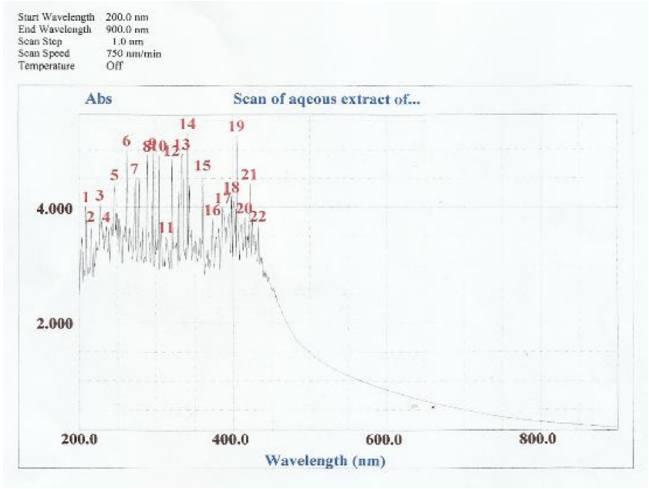

FIGURE 1 UV scan spectrum of the dye extract

interference between the co-adsorbed chromophores opening up the way for testing a multitude of other dye combinations.[24]

3.3 | GC-MS of the extract

Some of the chemical compounds identified in the *Alstonia boonei* leaf extract by GC-MS are shown in Table 2.

The spectrum of the relative abundance vs time of the components of the dye extract is shown in Figure 2.

TABLE 2 Result of GC-MS of the dye extract

Compound name	Elution time (min)	Relative molecular formula/M mass
2,6,10,14-tetramethyl hexadecane 2,6,10,15-tetramethylheptadecane 2-methyl decane	13.278	$C_{20}H_{42}$ (282.54) $C_{21}H_{44}$ (296.55) $C_{11}H_{24}$ (156.19)
13,14-diMethyl, pentadecanoate Methyl hexadecanoate	15.916	$C_{17}H_{34}O_2$ (270.457) $C_{17}H_{34}O_2$ (270.457)
Methyloctadec-9,12-dienoate	18.153	$C_{19}H_{34}O_2$ (294.47)
Methyloctadec-11-enoate Methyloctadec-9-enoate Methyloctadec-6-enoate	18.233	$C_{19}H_{36}O_2$ (296.495) $C_{19}H_{36}O_2$ (296.495) $C_{19}H_{36}O_2$ (296.495)
Neophytadiene Phytol 3,7,11,15-tetramethyl-hexadec-2-en-1-ol	18.416	$C_{20}H_{38}$ (278.524) $C_{20}H_{40}O$ (296.539) $C_{20}H_{40}O$ (296.539)
Methyl stearate	18.616	$C_{19}H_{38}O_2$ (298.511)
Linoleic acid	18.963	$C_{18}H_{32}O_2$ (280.452)
Octadeca-9,12-dienoic acid	19.211	$C_{18}H_{32}O_2$ (280.452)
Hexamethyl-tetra cosa-2,6,10,14,18,22-Hexaene (squalene)	27.823	$C_{30}H_{50}$ (410.73)
Olean-12-en-3-ol, acetate, (3.beta) 12-Oleanen-3-yl acetate, (3.alpha)	32.469	$C_{32}H_{52}O_2$ (468.766) $C_{32}H_{52}O_2$ (468.766)
Urs-12-en-24-oic acid, 3-oxo-methyl ester Urs-12-en-3-ol, acetate	32.750	$C_{31}H_{48}O_3$ (468.766) $C_{32}H_{52}O_2$ (468.766)

From the spectrum of the relative abundance of the various compounds in the extract identified in GS-MS against the elution time, it can be seen that the compound eluted at time 18.963 minutes linoleic acid is the

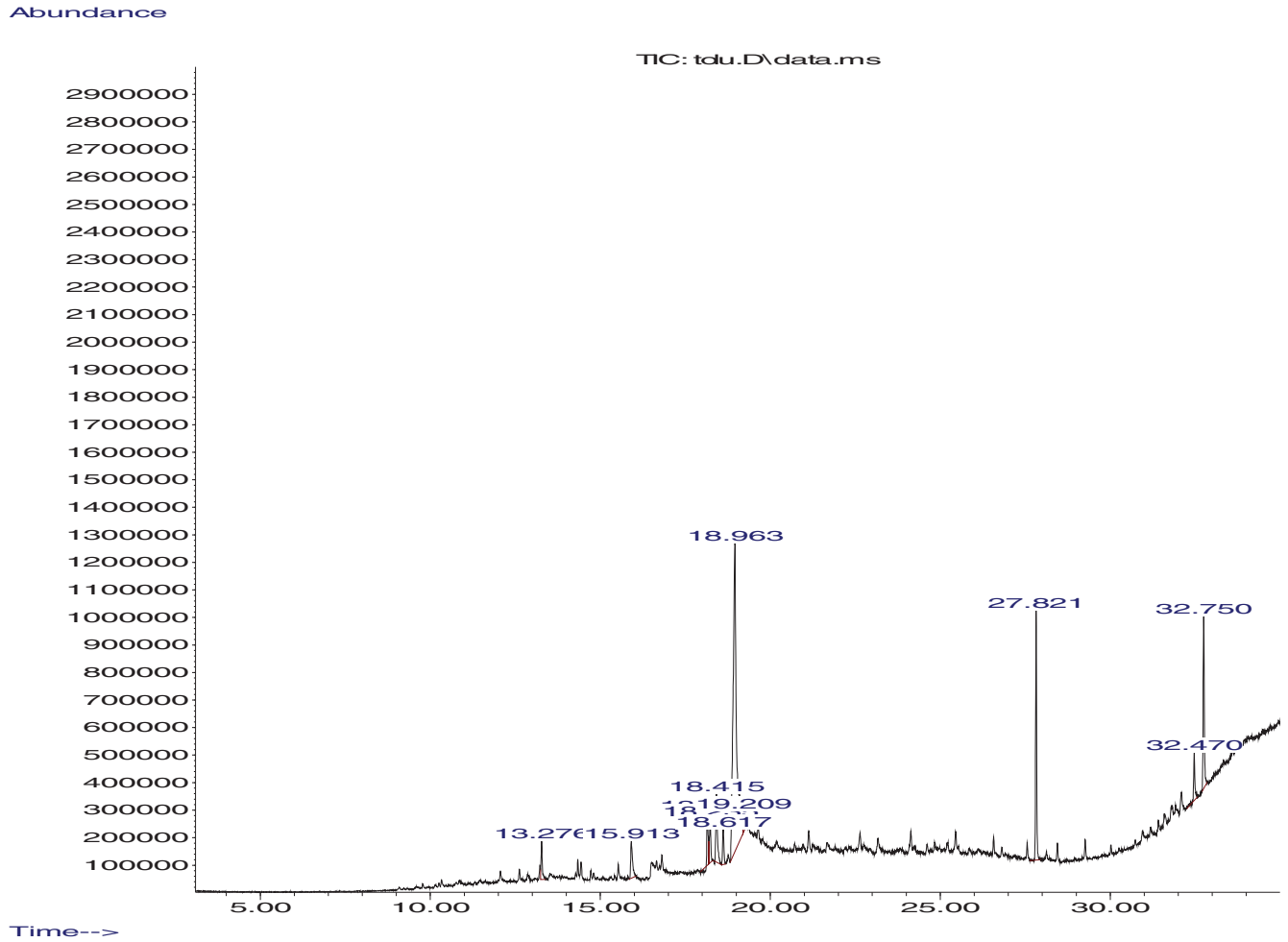

FIGURE 2 Chromatogram of relative abundance against elution time of the components in gas chromatography

most abundant component (52.83%), the compound eluted at 27.82 minutes hexamethyl-tetra cosa-2,-6,10,14,18,22-hexaene or squalene is the second most abundant (13.15%) closely followed by that eluted at 32.75 minutes Urs-12-en-24-oic acid, 3-oxo- (10.20%). These three components account for more than 76% of the components of the extract. The three major components of the extract are high molecular compounds with many JI-electrons, atoms and high conjugation capable of both absorbing and extending conjugation at the UV/visible region of the electromagnetic spectrum. This justifies the strong absorption at UV/visible region of the electromagnetic spectrum by the extract.[21-23]

From the result of the GC-MS of the sample also, it can be seen that besides the three major components, there are so many chemical components in the sample that are capable of absorbing electromagnetic radiation within the UV/visible region (10-780 nm).[24]

The ideal sensitizer for a single junction photovoltaic cell converting standard global AM 1.5 sunlight to electricity should absorb all light below a threshold wavelength of approximately 920 nm. In addition, it must also carry attachment groups such as carboxylate or phosphonate to firmly graft it to the semiconductor oxide surface.[25] Upon excitation, it should inject electrons into the solid with a quantum yield of unity. The energy level of the excited state should be well matched to the lower bound of the conduction band of the oxide to minimize energetic losses during the electron transfer reaction. Its redox potential should be sufficiently high that it can be regenerated via electron donation from the redox electrolyte or the hole conductor. Finally, it should be stable enough to sustain about 108 turnover cycles corresponding to approximately 20 years of exposure to natural light. Much of the research in dye chemistry is devoted to the identification and synthesis of dyes matching these requirements while retaining stability in the photo-electrochemical environment.[26] The attachment group of the dye ensures that it spontaneously assembles as a molecular layer upon exposing the oxide

film to a dye solution. The dominant molecules identified in *Alstonia boonei* contain many of these anchoring groups, which explain the relatively smooth absorption/chemisorption observed in DSC when it was soaked in the dye. This molecular dispersion ensures a high probability that, once a photon is absorbed, the excited state of the dye molecule will relax by electron injection to the semiconductor conduction band.[27] However, the optical absorption of a single monolayer of dye is weak, a fact that originally was cited as ruling out the possibility of high efficiency sensitized devices, as it was assumed that smooth substrate surfaces would be imperative in order to avoid the recombination loss mechanism associated with rough or polycrystalline structures in solid-state photovoltaic. This objection was invalidated by recognizing that the injection process produces electron in the semiconductor lattice, separated spatially from the positive charge carriers by the dye molecules, which are insulating in the ground state and hence provide a barrier for charge recombination.[28]

3.4 | Morphological characterization

3.4.1 | Film thickness

The thickness of sensitized TiO_2 film with dye at various pH values is the same 3.0 μm. However, it has been reported earlier in an experiment using TiO_2 film between 2.8 and 6.7 μm thicknesses gave good result.[29]

The thickness of 3.0 μm chosen for the work was because of the incubation time of the photoanode, which was 1 hour 30 minutes. This thickness was maintained for all the DSSCs at different dye pH values so as to maintain uniformity. The chosen incubation time was to avoid severe thermal cracking and high molecular agglutination and dye aggregation at higher incubation time due to the lightness of the chosen film thickness. Thomas et al reported that there is a sharp relationship between the film thickness of photoanode and the incubation period with the overall cell efficiency.[28] Hence there is always a point of optimization between the film thickness and the incubation, which is what was considered in the work.

3.4.2 | Cell active area

The active area of the cell sensitized with the dye was measured to be 0.4 cm^2. The area of all the cells is the same because the active area and the gum area of all the DSSC were screen printed from the same design.

3.4.3 | Scanning electron microscope micrograph image of the nanoporous TiO_2

Monograph images of the nanoporous TiO_2 film deposited on the FTO previously covered with a blocking layer at different resolutions and magnification are presented in Figure 3.

The scaling of the image for A, B, C and D are 30, 50, 30, and 100 μm, as shown by the scale at left-hand side at the bottom of the image. The working distance, which is the distance between the sample and the machine detector, is 134, 179, 701 and 500 μm, respectively. The electron accelerating voltage is 15 KV. From the figure, it can be seen that there was formation of mesoporous surface of the nanoparticles clustering on the film surface.[8,25,30]

The SEM image of *n*-TiO_2 film at various scales A, B, C, D in Figure 3 above shows that the film contains fine crystalline structure, which is good for absorption of dye molecules on the thin film of TiO_2. There are also contours that are developed during the annealing process of the photoanode. The prominent contour lines suggest that the annealing process lasted nearly beyond the required temperature. The implications this could have on the DSSC are leakage of the electrolyte after sealing and thermal ionization in severe condition.[28,31]

3.5 | XRD diffractogram of the Tio_2 nano film

Figure 4 shows the diffractogram pattern of the dye molecules absorbed on the TiO_2.

The sharp points indicate the forming of a material with high crystallinity. The points formed in TiO_2 are included in the anatase phase. From the diffractogram, it can be seen that dominant point is at 2θ: 25.32; 37.86 and 48.56. From the calculation, the average particle size was 78.34205 nm. The anatase phase has a higher photoactive ability compared with the rutile. It is caused by the larger surface area of the anatase compared with the rutile's, so that the per-unit active sides of the anatase are bigger. With the anatase phase, it is possible that the DSSC efficiency production can be increased. The absorbed dye molecules will further enhance the photo-activity of the anatase form, which inherently has a capacity of absorbing up to 20% to 35%.[26,32]

Anatase appears as pyramid-like crystals and is stable at low temperatures, whereas needle-like rutile crystals are dominantly formed at high-temperature processes. Single crystals of TiO_2 also have a rutile structure. The densities are 3.89 and 4.26 g/cm^3 for anatase and rutile, respectively. Rutile absorbs approximately 4% of the

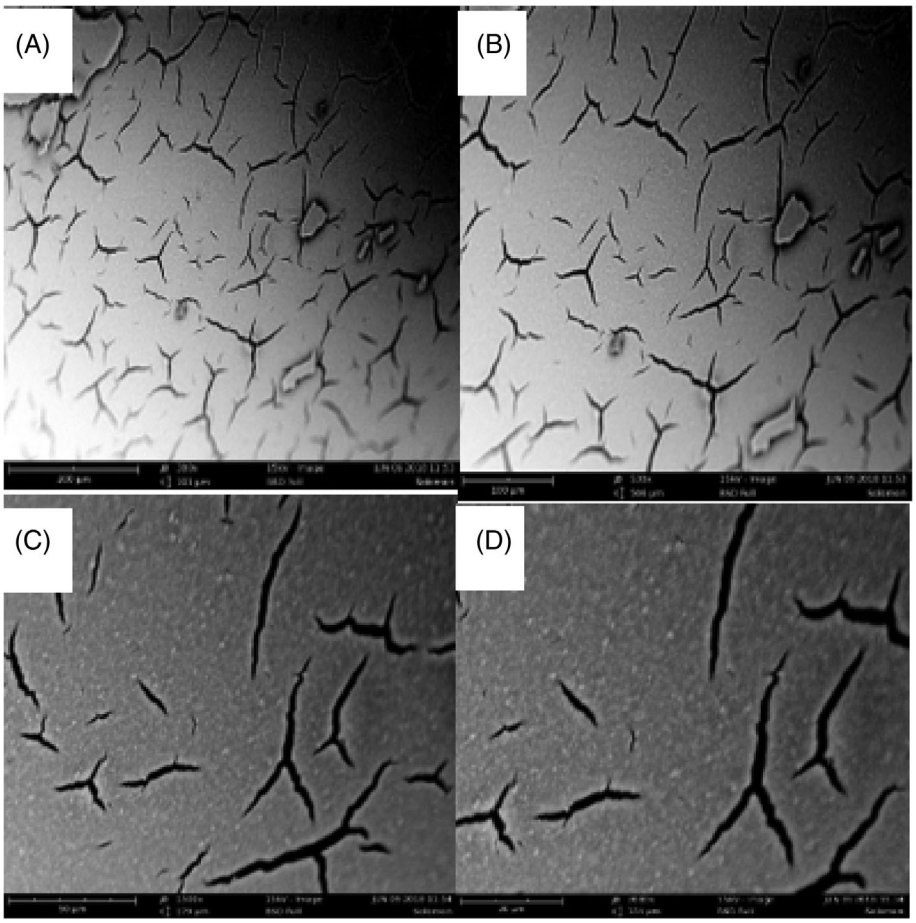

FIGURE 3 SEM micrograph of the n-TiO_2 film

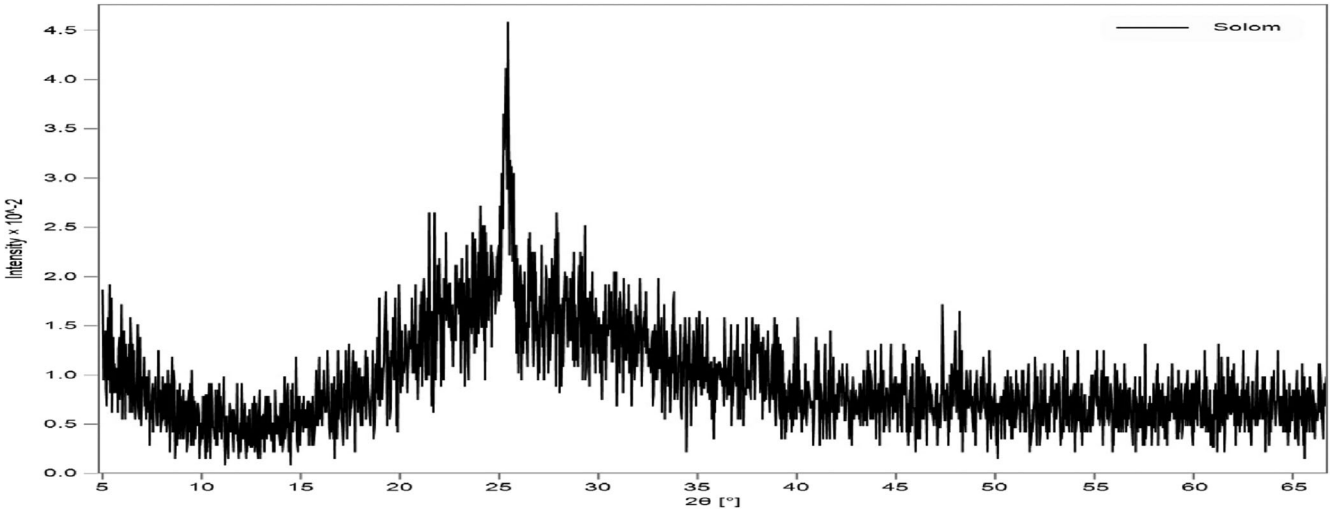

FIGURE 4 XRD spectrum of peak intensity vs diffraction angle (2θ)

incoming light in the near-UV region, and band gap excitation generates holes that act as strong oxidants reducing the long-term stability of the DSSCs. The third crystalline form of TiO_2, brookite, is difficult to produce and it is, therefore, not of practical interest for the DSSCs. The band gaps of the crystalline forms are 3.2 eV (the absorption edge at 388 nm) for anatase and 3.0 eV (the absorption edge at 413 nm) for rutile. This gives the anatase phase a comparative advantage in DSSC technology.[4]

3.6 | Optical characterization of DSSC

The result of the absorbance spectrum of DSSC at different dye pH values is shown in Figure 5.

DSSC at dye pH 3.00 shows the highest absorbance at all the regions of the electromagnetic spectrum. This is closely followed by the cells at pH values 5.68 and 1.30, whose absorbance is interwoven at all the examined wavelengths. The DSSCs absorb well ultraviolet (UV), visible and near infrared (NIR) in the wavelength range of 300 to 1100 nm with absorption maxima (λ_{max}) at wavelengths 310, 477, 750, 760, and 1035 nm within the plotted area. The non-sensitized TiO_2 film has the lowest absorption in all the regions of the electromagnetic spectrum, as shown above. This shows that the dye photosensitizer enhances the ability of the TiO_2 film in absorbing and harvesting UV/visible light.[8,27,33]

Table 3 shows the absorption maxima of UV/visible light by dye/DSSC and pure TiO_2. This implies that the DSSC at dye pH 3.00 has the highest absorption peak (1.963).

Figure 6 shows the comparative plot of transmittance at various pH values and pure TiO_2 layer.

The spectra of optical transmittance of all the DSSCs show a similar pattern. Notable from the spectra is the fact that they show very low optical transmittance (<10%) within the UV/visible region. Each of their transmittance progressively increased as the wavelength increases. The TiO_2, on the other hand, show higher transmittance at the UV/visible region (>40%). As the wavelength increased, the transmittance reached a steady maximum of approximately 99% at wavelength 550 nm and above.[17,27,34] The peak transmittance of the DSSC is presented in Table 4.

Figure 7 shows the relationship between the photon energy and wavelength as calculated.[27]

From the plot, as the wavelength increases, photon energy decreases from the UV to near-IR region. This is in tandem with the Max Planck equation of photo-energy and wavelength. This implies that the light of high energy gamma and UV light has a short wavelength while those with low energy (near-IR) have a longer wavelength.[18]

Band gaps of TiO_2 nano film of DSSC sensitized with dye at various pH values are presented in Figures 8A-E.

From the graphs, the band gaps were measured and recorded in Table 5.

From the table, it is clear that modifying the dye pH has an effect on the band gap of the semiconductor showing that it has sensitizing ability and hence can enhance

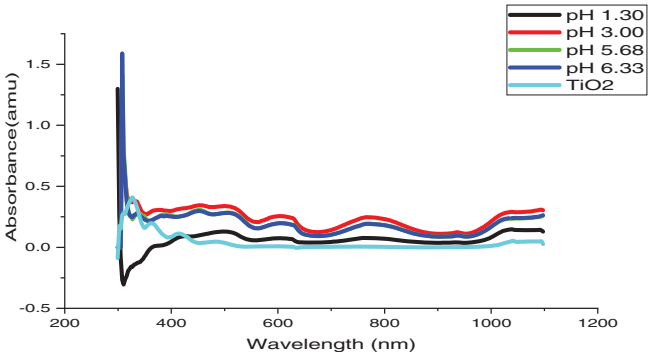

FIGURE 5 Plot of absorbance against wavelength of DSSC at various dye pH values

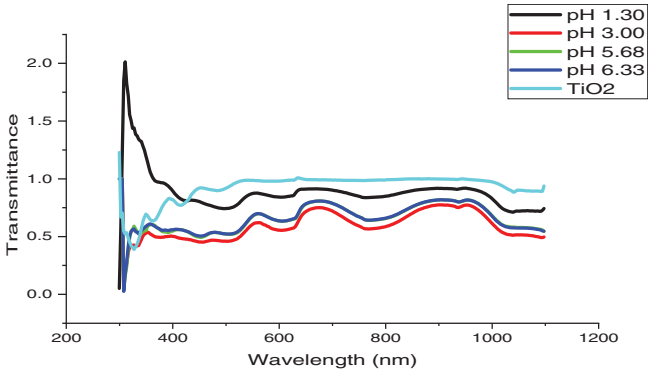

FIGURE 6 Comparative plot of transmittance at various pH values and pure TiO_2 layer

TABLE 3 Absorption maxima of UV/visible light by the nDSSCs

Dye pH	Maximum absorbance (A.U.)	Wavelength (nm)
1.30	1.298	299.50
3.00	1.963	307.84
5.68	1.413	307.84
6.33	1.589	307.84
Pure TiO_2	0.410	327.30

TABLE 4 Table of transmittance peaks of DSSC at different dye pH values

Dye pH	Maximum transmittance (%)	Wavelength (nm)
1.30	81	990.50
3.00	80	1000
5.68	83	700 and 950
6.33	80	700 and 900
Pure TiO_2	99	550 to 1100

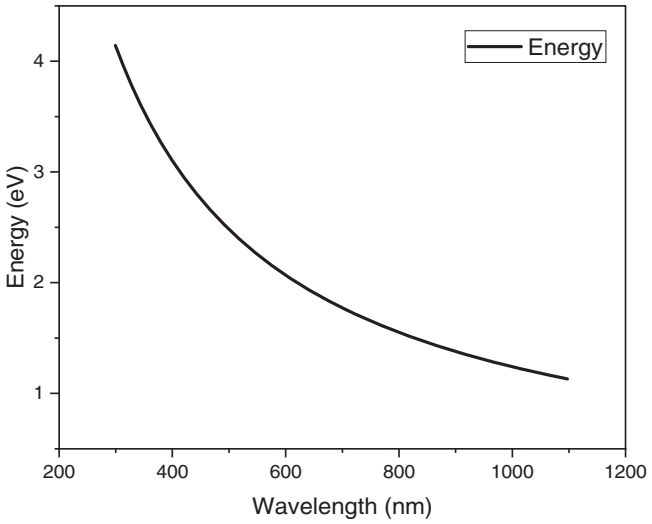

FIGURE 7 Plot of energy vs wavelength

DSSC harvesting and conversion efficiency of the cell.[18,34]

3.7 | Electrical characterization and discussion

3.7.1 | Sheet resistance

The average sheet resistance of the nDSSCs was measured and is presented in Table 6.

In DSSC technology, because the cell is an ohmic material, other factors remaining constant, the current flow in the DSSC is inversely related to resistance. The lower the resistance, the higher the expected current density of the DSSC.[18,34,35]

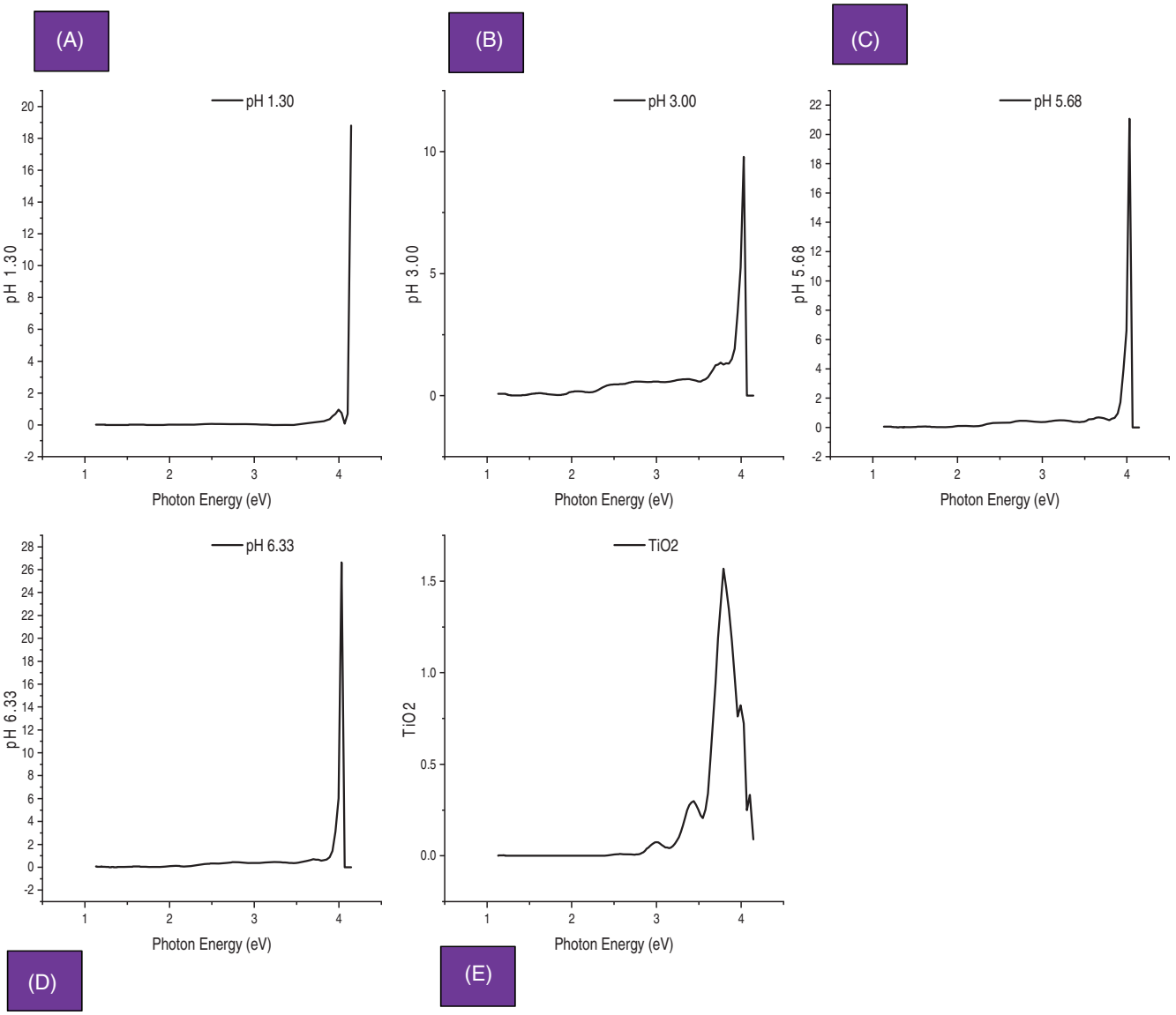

FIGURE 8 (A-E) Plot of absorption coefficient squared vs photon energy at dye pH1s 1.30, 3.00, 5.68, 6.33 and pure TiO_2 film

3.7.2 | I-V characteristics of the DSSCs

The result of the current-voltage properties of the DSSCs at different pH values measured are present in Table 7 and plotted in Figure 9.

An efficiency of 0.23% was obtained for DSSC at pH 1.30, the DSSC at dye pH 3.00 gave an efficiency of 0.98%, while the DSSC made at dye pH 5.68 gave an efficiency of 0.97%, and efficiency of 0.05% was obtained for the cell without pH modification as shown in Table 7.

This shows that the modification of the pH of dye to be used as solar sensitizer has an effect on the sensitizing ability.[8,21] The table presented above shows that the optimum pH that gave the highest cell efficiency among the studied pH values is pH 3.00, this was followed by the DSSC at dye pH 5.68 while the least is the DSSC made at dye's natural pH. The very low efficiency obtained from the cell at dye pH 1.30 (highly acidic environment) could be due to degradation of dye molecules at very low pH (high acidity), which is very far from the natural pH of the dye (pH 6.33).[8,18,36,37] On the other hand, the increased efficiency obtained from the DSSC at dye pH 3.00 (mildly acidic) and that at dye pH 5.68(weakly acidic) corroborated the earlier assertion that natural dyes absorb ultraviolet/visible radiation better at fairly acidic environment.[5,31] This phenomenon is also illustrated in photosynthesis in green plants. The result shows that *Astonia boonei* is a good photosensitizer compared with other natural dyes already studied in the literature.

The efficiency of all the cells at different photosensitizer dye pH is relatively low compared with some other natural and synthetic dyes already studied in the literature.[10,11,18,21] There are two major explanations for this low conversion efficiency. First is that the efficiency of DSSCs does not depend solely on a single factor but rather on various factors like electrolyte system, type and nature of active and counter electrodes, design and structure of the DSSC, etc. The key noticeable factors that are responsible for the low efficiency and stability of the DSSCs in this work include non-optimized dark current, poor performance of dye in NIR region, poor contact between the electrodes, which is evident in observed leakage of electrolyte over time, low volatility and poor viscosity of electrolyte and degradation of

TABLE 5 The band gaps obtained for DSSCs at various dye pH values

	DSSC pH	Band gap obtained (eV)
1	1.30	4.15
2	3.00	3.70
3	5.68	3.83
4	6.33	3.81
5	Pure TiO_2 film	3.50

TABLE 6 Average sheet resistance of DSSCs at different pH values

	DSSC pH	Average sheet resistance(Ω/sq)
1	1.30	16.41
2	3.00	13.83
3	5.68	14.06
4	6.33	14.77

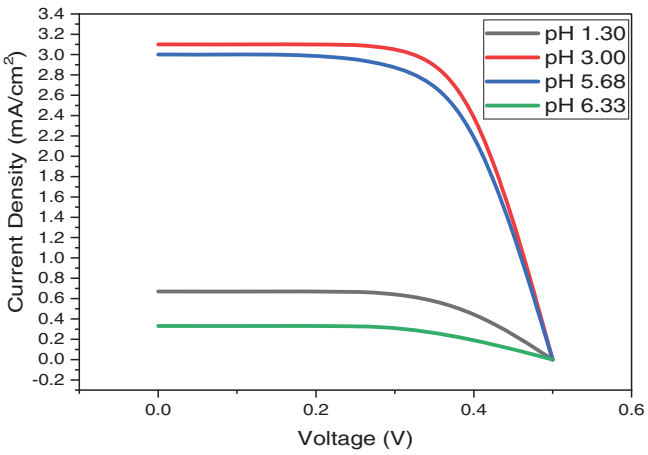

FIGURE 9 Graph of I-V curve of DSSCs at different pH

TABLE 7 I-V characteristics of the DSSCs

I-V Characteristics	DSSC of pH 1.3	DSSC of pH 3.0	DSSC of pH 5.68	DSSC of pH 6.33
J_{mp} (mA/cm^2)	0.50	3.00	2.55	0.20
V_{mp} (volt)	0.46	0.34	0.38	0.26
J_{sc} (mA/cm^2)	0.67	3.10	3.00	0.33
V_{oc} (volt)	0.49	0.47	0.48	0.51
FF	0.70	0.67	0.67	0.31
η	0.23	0.98	0.97	0.05

electrolyte properties due to exposure to and subsequent absorption of the UV light. However, for further studies, the efficiency and stability of the DSSCs can be improved by; improving the surface properties and morphology of the semiconductors to reduce the dark current, using additives for dyes and electrolytes that enhance their properties, improving the mechanical contact or adhesion between the active and counter electrode, and developing, using low volatile and moderately mobile electrolyte to enhance adequate charge transfer rate. Secondly, it was intended to ascertain if varying the pH of a particular dye used as a photosensitizer can produce different results in terms of solar activity and, by extension, show different efficiency.[10,11] The underlying principle here is that all the cells at different dye pH values were subjected under similar and same condition so that any variation in efficiency is due to the varied pH of the sensitizing dye. All the other factors that affect DSSC efficiency, which were neglected or rather kept constant, could be the reason for the low efficiency obtained at the end but this does not in any way invalidate the work since the purpose of the work was achieved and the research hypothesis that dye pH affects the ability of the dye when used as a photosensitizer in DSSCs. The significance is that even those synthetic and natural dyes that have in other works showed higher efficiency can be further improved by trying them at different pH values. Generally, it is known that silicon-based solar cells are more efficient than synthetic dye solar cell, and the latter is, in turn, more efficient than natural DSSC; more efforts are on improving the efficiency of nDSSCs due to the inherent comparative advantage it maintains over the others.[2,12,14] To overcome this challenge, plenty of experimental research studies are focusing on different factors that affect the solar radiation sensitivity and absorption by dyes to see how best they can be varied and combined in order to obtain measurable and comparable light conversion efficiency from natural dyes. This explains why researchers are picking on various variables in nDSSCs like electrolytes, film thickness, sintering temperature, metallic oxide layer, doping material, sputtering method, strength and exposure time to solar stimulator, counter electrode catalyst, etc, to see how optimum conditions can be obtained and best combined to get nDSSCs that will compete with solid-state silicon-based solar cell and pave the way for full commercialization of this generation of a voltaic cell. Further work may be in line with multiple dyes in DSSC, multiple junction DSSC and graded junction DSSC. Here, different dye capabilities may be systematically arranged to enhance interface carrier transfer for better overall efficiency of the multiple graded heterostructure DSSC.

4 | CONCLUSION

DSSCs using the natural dye from stool wood leaves (*Alstonia boonei*) were successfully fabricated using screen printing method at adjusted dye pH values. The DSSCs were characterized and the active cell area, film thickness of 3.0 μm and efficiencies of 0.23%, 0.98%, 0.97% and 0.05% were obtained for DSSCs at dye pH values of 1.30, 3.00, 5.68 and unmodified (6.00) dye DSSC, respectively. These compared well with previous results from research, which showed efficiencies of 0.59, 0.12, 0.22, 0.20, 0.07, 0.34, 0.13, *Punica granatum* (Pomegranate), *Jathropha curcas* Linn (Botuje), *Anethum graveolens*, Arugula, *Petroselinum crispum* (Parsley), *Herba artemisiae scopariae* (spinach), respectively, to mention but a few.[38]

The extent of modification of band gap of the TiO_2nanoporous layers at various dye pH values was examined and showed improved ability to absorb light in the visible, ultraviolet and NIR regions. This shows that *Alstonia boonei* dye is a good DSSC sensitizer and more so when the pH is modified to an optimum level.

To this end, if optimized and harnessed, DSSC with *Alstonia boonei* dye as a sensitizer will present clean, cheap and renewable alternative energy source to fossil fuel. This has a very big environmental advantage and economic prospect.[35,39]

ORCID

Uche E. Ekpunobi https://orcid.org/0000-0003-2079-8470

REFERENCES

1. Desalegn JG, Sisay TA, Teketel YA. Dye sensitized solar cells using natural pigments from five plants and quasi-solid state electrolyte. *J Braz Chem Soc*. 2015;26(1):92-101.
2. Hagfeldt A, Boschloo G, Sun L, Kloo L, Pettersson H. Dye-sensitized solar cells. *Chem Rev*. 2015;110(11):6595-6663.
3. Gratzel M. Dye sensitized solar cells. *J Photochem Photobiol C*. 2003;4(2):145-153.
4. Prabavathy N, Shalini S, Balasundaraprabhu R, Velauthapillai D, Prasanna S, Muthukumarasamy N. Enhancement in the photo stability of natural dyes for dye sensitized solar cells (DSSC) application: a review. *Int J Energy Res*. 2017;41(10):1372-1396.
5. Senthamarai R, Ramakrishnan V, Palanisamy B, Kulandhaivel S. Synthesis of TiO_2 nanostructures by green approach as photoanodes for dye-sensitized solar cells. *Int J Energy Res*. 2020;45:3089-3096.
6. Younas M, Gondal MA, Mehmood U, Harrabi K, Yamani ZH, Al-Sulaiman FA. Performance enhancement of dye-sensitized solar cells via cosensitization of ruthenizer Z907 and organic sensitizer SQ2. *Int J Energy Res*. 2018;42(12):3957-3965.
7. Lai F, Yang J, Hsu Y, Kuo S. Omnidirectional light harvesting enhancement of dye-sensitized solar cells decorated with two-

dimensional ZnO nanoflowers. *J Alloys Comp*. 2020;815: 152287.
8. Isah KU, Ahmadu U, Idris A, et al. Betalain pigments as natural photosensitizers for dye-sensitized solar cells: the effect of dye pH on the photoelectric parameters. *Mater Ren Sustainable Energy*. 2015;4(1):1-5.
9. Sie CZW, Ngaini Z. Incorporation of kojic acid-azo dyes on TiO_2 thin films for dye sensitized solar cells applications. *J Sol Energy*. 2017;2017:1-10.
10. Ghann W, Kang H, Sheikh T, et al. Fabrication, optimization and characterization of natural dye sensitized solar cell. *Sci Reports*. 2017;7(1):41470.
11. Prabavathy N, Shalini S, Balasundaraprabhu R, et al. Algal buffer layers for enhancing the efficiency of anthocyanins extracted from rose petals for natural dye-sensitized solar cell (DSSC). *Int J Energy Res*. 2018;42:(2):790-801.
12. Al-Alwani MAM, Mohamad AB, Ludin NA, Kadhum AH, Sopian K. Dye-sensitised solar cells: development, structure, operation principles, electron kinetics, characterisation, synthesis materials and natural photosensitisers. *Ren Sust Energy Rev*. 2016;65:183-213.
13. Synfinar R, Gomesh N, Irwanto M, Areq M, Irwan YM. Chlorophyll pigments as nature based dye for dye-sensitized solar cell (DSSC). *Energy Procedia*. 2015;79:896-902.
14. Kalaichelvi BK, Dhivya SM. Screening of phyto constituents, UV-VIS Spectrum and FTIR analysis of *Micrococca mercurialis* (L.). *Int J Herb Med*. 2017;5(6):40-44.
15. Hernandez AR. Natural pigment based dye sensitized solar cells. *J Appl Res Technol*. 2012;10:38-47.
16. Green M. Solar cells: Operating principles, technology and system applications. *J. Sol. Energy*. 1982;28(5):447.
17. Bignozzi CA. Recent developments in the design of dye-sensitized solar cell components. Workshop on Nanoscience for Solar Energy Conversion, ICTP, Trieste; 2008;1-67.
18. Oviri OK, Ekpunobi AJ. Fabrication and characterization of dye-sensitized solar cell using Anarcadium occidentale sensitizer. *Adv Appl Sci Res*. 2012;3(5):3390-3395.
19. Jiao Y, Mao L, Liu S, et al. Effects of meta or Para connected organic dyes for dye-sensitized solar cell. *Dyes Pigm*. 2018;158: 165-174.
20. Singh LK, Koiry BP. Natural dyes and their effect on efficiency of TiO_2 based DSSCs: a comparative study. *Mater Today: Proc*. 2018;5(1):2112-2122.
21. Socrates G. *Infrared and Raman Characteristic Group Frequencies: Tables and Charts*. 3rd ed. West Sussex, England: John Wiley & Sons; 2004;1-364.
22. Gong R, Sun Y, Chen J, Liu H, Yang C. Effect of chemical modification on dye adsorption capacity of peanut hull. *Dyes Pigm*. 2005;67(3):175-181.
23. Stejskal J, Gilbert RG. Polyaniline. Preparation 0f a conducting polymer(IUPAC Technical Report). *Pure Appl Chem*. 2002; 74(5):857-867.
24. Silverstein RM, Bassler GC, Morrill TC. *Spectroscopic Identifications of Organic Compounds*. 4th ed. New York: John Wiley and Sons; 1981.
25. Al-Alwani AM, Al-Mashaan ABSA, Abdullah MF. Performance of the dye sensitized solar cells fabricated using natural dyes from *Ixoracoccinea* flowers and *Cymbopogonscho ennanthus* leaves as sensitizers. *Int J Energy Res*. 2019;43:1-11.
26. Atli A, Atilgan A, Yildiz A. Multi-layered TiO_2 photoanodes from different precursors of nanocrystals for dye-sensitized solar cells. *Sol Energy*. 2018;173:752-758.
27. Hao S, Wu J, Huang Y, Lin J. Natural dyes as photosensitizers for dye sensitized solar cells. *Sol Energy*. 2006;80:209-214.
28. Thomas K, Dimas K, Dass MP. Use of plant pigment extracted from *Euphorbiacotinifolia* leaf for dye sensitized solar cell (DSSC). *J Chem Soc Nigeria*. 2019;44(4):619-628.
29. Waita SM, Mwabora JM, Aduda BO, Niklasson G. A performance of dye-sensitized solar cells. *Asian J Sci Technol*. 2006; 7(2):106-119.
30. Mulati DM, Timonah NS, Bjorn W. The absorption spectra of natural dyes and their suitability as a sensitizer in organic solar cell application. *Org Sol Cells*. 2012;14:45-60.
31. Venkatraman MR, Muthukumaramy S, Selvakumar P, et al. UV-aided graphene oxide reduction by TiO_2 towards TiO_2/reduced graphene oxide composites for dyesensitized solar cells. *Int J Energy Res*. 2020;45:17220-17232.
32. Negese Y, Delele W, Abebe R. Natural dye as light-harvesting pigments for quasi-solid-state dye-sensitized solar cells. *Mater Renewable Sustainable Energy*. 2016;5:13.
33. Gokilamani N, Muthukumarasamy N, Thambidurai M, Ranjitha A, Velauthapillai D. Utilization of natural anthocyanin pigments as photosensitizers for dye-sensitized solar cells. *J Sol-Gel Sci Tech*. 2013;66(2):212-219.
34. Ugwu LU, Ozuomba JO, Ekwo PI, Ekpunobi AJ. The optical properties of anthocyanin-doped nanocrystalline-TiO_2 and the photovoltaic efficiency on DSSC. *Der Chem Sin*. 2015;6(11):42-48.
35. Reijnders L. Design issues for improved environmental performance of dye sensitized and organic nano-particulate solar cells. *J Cleaner Prod*. 2010;18:307-312.
36. Al-Alwani MAM, Mohamad AB, Ludin NA, Kadhum AH, Mukhlus A. Application of dyes extracted from *Alternanthera dentata* leaves and *Musa acuminata*bracts as natural sensitizers for dye-sensitized solar cells. *Spectrochim Acta A Mol Biomol Spectrosc*. 2018;192:487-498.
37. Atli A, Atilgan A, Altinkaya C, Ozel K, Yildiz A. St. Lucie cherry, yellow jasmine, and madder berries as novel natural sensitizers for dye-sensitized solar cells. *Int J Energy Res*. 2019; 43(8):3914-3922.
38. Agarwal P, Yusuf M, Khan SA, Prasad L. In: Yusuf M, ed. *Bio-Colorants as Photosensitizers for Dye Sensitized Solar Cell (DSSC) In: Handbook of Renewable Materials for Coloration and Finishing,*. Beverly, MA: Scrivener Publishing LLCm; 2018:294-315.
39. Shalini S, Balasundaraprabhu S, Prasanna R, Tapas K, Senthilarasu S. Review on natural dye sensitized solar cells: operation, materials and methods. *Renewable Sustainable Energy Rev*. 2015;51:1306-1325.

How to cite this article: Ekpunobi UE, Ogbuefi SI, Ekpunobi AJ. Dye pH effect on photoelectric parameters of natural photosensitizer pigment extracted from *Alstonia boonei* for dye-sensitized solar cells. *Int J Energy Res*. 2021;1-12. doi:10.1002/er.7307